RESEARCH ARTICLE

Echo character mapping and depositional processes on the western Svalbard continental margin

Niamh I. Doherty & John A. Howe

Scottish Association for Marine Science & the University of the Highlands and Islands, Dunbeg, Oban, Scotland, UK

Abstract

An echo character mapping study of the western Svalbard continental margin, based on ca. 3980 km of archived sub-bottom profile data, is presented. Four distinct echo character types are recognized. Type I is found on the continental slope and in the fjords as thin, irregularly parallel, sub-bottom reflectors, interpreted as glaciomarine plumes, turbidites and other features resulting from low-energy depositional processes. Type II occurs in the deeper water regions of the slope and basins as continuous, well-stratified, parallel reflectors that are interpreted as hemipelagites, distal turbidites and contourites. Type III, found only on the shelf, comprises continuous, highly reflective reflectors that are interpreted as coarse-grained sediments or exposed bedrock. Type IV occurs in fjords and shelf regions and is characterized by a single sub-bottom reflector with a transparent unit; it is interpreted as poorly sorted glacial diamict. This study also mapped numerous seabed features, including debris flow lobes, channel systems, pockmarks and gas chimneys. It illustrates how echo character mapping furthers our understanding of processes on the margin and contributes to reconstructing palaeoceanographic and palaeoclimatic conditions.

Keywords

Sub-bottom profiles; sedimentary processes; Svalbard–Barents Sea Ice Sheet; sea floor morphology; seismic facies; Arctic

Correspondence

John A. Howe, Scottish Association for Marine Science & the University of the Highlands and Islands, Dunbeg, Oban, PA37 1QA, Scotland, UK. E-mail: john.howe@sams.ac.uk

Abbreviations

GDF: glacial debris flow
IBCAO: International Bathymetric Chart of the Arctic Ocean (version 4)
KCS: Kongsfjorden Channel System
LGM: Last Glacial Maximum
SBP: sub-bottom profile
SBPr: sub-bottom profiler
TOPAS: topographic parametric sonar

Introduction

Seafloor sediment types have different characteristic acoustic properties that affect how they scatter and absorb sound waves on the account of their variations in density and therefore acoustic impedance. Hamilton (1956) recognized that sediment acoustic properties can be examined by echo sounder. Modern seabed acoustic surveys use high-resolution SBPrs, such as TOPAS, to infer different sediment compositions and processes in the marine environment. This technique typically utilizes the elapsed two-way travel time between generation and detection by transducers of acoustic pulses from different acoustic boundaries within seafloor sediments (Davies et al. 1999). Damuth (1975, 1978, 1980) developed the first acoustic classification of deep-sea environment sediments on the basis of inferences from echo sounder results. Variation in acoustic characteristics has been categorized, for example, by Damuth & Hayes (1977), according to criteria of bottom morphology, roughness, acoustic penetration and continuity of subsurface reflectors. Researchers continue to widely apply this technique as a fundamental part of geophysical studies in deep-sea and shallow marine environments (e.g., Domzig et al. 2009; Maestro et al. 2021).

SBPs can indicate a variety of physical processes that influence sediment records on high-latitude continental margins, such as climate processes, sea-level change, ice-sheet dynamics and oceanographic regimes (Chauhan et al. 2016). These can vary on temporal and spatial scales (McCave 2002). The spatial resolution to which sedimentary processes and their regional influences are inferred largely depends on the availability of seismic SBP lines, along which the distribution of different echo types is mapped (Damuth 1978). Little of the World Ocean has SBP coverage, and there are special challenges to acquisition in high-latitude seas prone to sea ice (Jakobsson et al. 2016). The limited existing and accessible SBPr data, including the archived legacy data sets used in this study, are important for better understanding the depositional and erosional processes at high latitudes.

Through a detailed examination of reprocessed existing TOPAS SBPr data, this study presents an extensive acoustic echo character classification map that is used to infer sedimentary processes on the high-latitude western Svalbard continental margin. Mass transport, erosional processes and indicators of gas or fluid flow seepage are among the processes and features inferred from the echo types and their associated occurrences.

Citation: *Polar Research* 2025, *44*, 10847, http://dx.doi.org/10.33265/polar.v44.10847

Regional setting

Geology and physiography

The glaciated continental margin of western Svalbard is the focus of this study. During the Miocene (ca. 17.5 Mya), the opening of the Fram Strait began with the separation of Greenland from Svalbard. This initiated sediment accumulation on the north-western Svalbard margin (Jakobsson et al. 2007). Plate tectonics drove this spreading, and the active mid-ocean ridge axis of the Molloy and Knipovich ridges was near Svalbard (Vorren et al. 1998). The margin's depositional history, principally the multiple glaciations of the Svalbard–Barents Sea Ice Sheet, has produced a diversity of depositional facies on the margin (Alexandropoulou et al. 2021). During the Quaternary, glaciations were the major process of sediment erosion and transport across the shelf to the slope (Dowdeswell et al. 1998). The most recent advance of the palaeo-Svalbard–Barents Sea Ice Sheet was initiated 32–30 Kya, with ice margins advancing over Svalbard and its present-day coastline (Hughes et al. 2016). Ice advance to the shelf break during the LGM occurred about 24 Kya (Jessen et al. 2010), fluctuating around peak ice-covered area size for several thousand years before the onset of deglaciation (Hughes et al. 2016).

Relatively shallow banks (50–100 m water depth) separated by deeper (200–400 m) cross-shelf glacial troughs as seaward continuations of the fjords characterize the morphology of the Barents Sea shelf, with the archipelago of Svalbard representing its most north-western extent (Nilsen et al. 2016). Under full glacial conditions, fast-flowing ice streams extended out to the shelf break and sculpted glacial troughs (Damuth 1978). These include the Kongsfjordrenna, Isfjordrenna and Bellsund glacial troughs. Ice streams draining within glacial troughs from major fjord systems, such as Kongsfjorden and Krossfjorden, supplied large volumes of sediment to the outer shelf over successive glaciations (Landvik et al. 2005). Repeated slope failures of these unstable deposits on the upper slope led to the development of stacked GDF lobes (Dowdeswell et al. 1998). GDFs can form large fan systems—called trough mouth fans (Vorren et al. 1998)—that are regional prograding features of the shelf break (Forwick et al. 2015).

Sediment deposition on the western Svalbard margin is strongly linked with interglacial–glacial cycles (Lucchi et al. 2024). Fine-grained muds from suspension settling of glacial meltwater, interlaced with coarser ice-rafted debris, occur in fjords during interglacial conditions and are subsequently eroded and transported offshore during glaciations (Dowdeswell et al. 1998). During glacial conditions, upper continental slope regions are deposited with GDFs (Elverhøi et al. 1998), with inter-fan regions having reduced sedimentation by ice and more intermittent slope failures (Solheim et al. 1998). More recently, during the Holocene, ice-distal slopes are draped in fine-grained glaciomarine and hemipelagic sediments and sediment drift deposits, originating either from suspension settling or current modification (Andersen et al. 1996).

Widespread gas or fluid seepage from sediment deposits occurs along the western Svalbard margin (Mau et al. 2017). This includes the contourite drift deposit at Vestnesa Ridge first reported by Vogt et al. (1994), with subsequent studies identifying both active and dormant regions of gas or fluid seepage occurrence in the region (e.g., Bünz et al. 2012). Features in seismic data that indicate fluid flow include transparent units, bright spots, gas chimneys and acoustic blanking on SBPs alongside—as seabed expressions—pockmarks, seabed domes and mud diapirs (Judd & Hovland 1992).

Oceanography

The Fram Strait opening connected the Arctic Ocean with the Nordic Seas (Rudels et al. 2000). This produced the recent, northward advection of warm, saline Atlantic Water—the West Spitsbergen Current—that is bathymetrically steered along the western Svalbard upper continental slope (Bensi et al. 2019). This is countered by the south-directed East Greenland Current in the western Fram Strait. In the north-western Fram Strait, the West Spitsbergen Current enters the Arctic Ocean as two currents: the Yermak Slope Current, contouring west and northwards at depth along the Yermak Plateau; and the North Spitsbergen Current, flowing more shallowly across the Yermak Plateau before continuing north and east of Svalbard (Rudels et al. 2000). The West Spitsbergen Current has been a major source of transport and modification of sediments on the margin for about the last 11 My (Eiken & Hinz 1993; Forwick et al. 2015). This current is also responsible for the construction of contourite drifts along the continental slope west of Svalbard (Rebesco et al. 2013).

Materials and methods

Sub-bottom profiling using TOPAS

High-resolution TOPAS data, covering 3980 km, were collected by the UK polar research vessel RRS *James Clark Ross* during three cruises: JR75 in 2002, JR127 in 2005 and JR219 in 2010. The TOPAS system used a hull-mounted transducer array generating a single, narrow beam following the ship track. The profiler was operated

Citation: *Polar Research* 2025, *44*, 10847, http://dx.doi.org/10.33265/polar.v44.10847

using a chirp (1.5–5 kHz) SBP source with additional secondary frequency bursts (2800 Hz). So the SBPr data could be georeferenced, the ship tracks and SBP lines were associated with specific trace time stamps. Data were archived at the Scottish Association for Marine Science and the British Antarctic Survey, both in analogue format on thermal paper and digitally in TOPAS raw format. Analysis of the data collected by each cruise utilized a combination of both data storage formats.

Software and processing

Version 2.1.2 of the TOPAS SBP system was supplied by the British Antarctic Survey. Alongside studying the SBPr data analogically using the thermal paper rolls, the TOPAS raw file format was converted to the SEG-Y standard format (developed by the Society of Exploration Geophysicists) to enable viewing with SeiSee (version 2.22.2) software. This required the TOPAS raw data to be re-processed in the Kongsberg TOPAS MMI SW (version 3.2) software system. Polygons and symbols, representing high-resolution features, were mapped in QGIS (version 3.28.10).

Positioning uncertainty

Since the SBPr data were derived from several cruises, minor mismatches in data acquisition and processing between profiles were unavoidable. This included, for example, the variation in trace time-stamp resolution between digital and analogue formats and between cruises—from <15 seconds for JR129 to 60 seconds for JR75 and JR127. This may have resulted in variation between cruises in the recorded accuracy of the positioning of the ship's SBP, with larger time steps requiring a greater assumption of a constant ship speed between time stamps. The impact of minor geographical errors in this study was minimized where possible.

Broad-scale echo character mapping

The construction of a broad-scale map of the distribution of different echo characters across the Svalbard margin was based on the approach of Damuth (1975, 1978, 1980). The following steps were conducted: (1) general SBP echo characters were assessed for the region; (2) interpretable SBPr data were subdivided into echo types, based on the observed acoustic character; (3) echo types were mapped along the ship tracks; (4) echo characteristics were subsequently inferred between track lines using a correlation with contour lines and the IBCAO (Jakobsson et al. 2020). The discrete classification of echo types is comparable to similar studies, such those by Damuth (1978), Pudsey & Howe (1998) and—pertinent to Svalbard—Gerbhardt et al. (2011). Resolution varies depending on availability of SBPr lines within the region. Distinct echo character type sections with lengths shorter than 2 km along the ship track line were mapped as separate polygons. The maximum penetration was about 35 m, based on an assumed P-wave seismic velocity for glaciomarine deposits of 1600 ms^{-1} (see Orsi & Dunn 1991; Aarseth 1997).

Geomorphological features mapping

The morphological features mapped across the study area are defined as any mass transport, gas or fluid flow or erosional feature with a minimum length of 0.5 km. Features were identified using a combination of SBPr data and IBCAO bathymetry (Jakobsson et al. 2020). Features identified included GDFs, pockmarks and chimneys; bathymetry and slope-aspect mapping were used to interpret a channel system. Overlaying these features within the broad-scale echo character map allowed for correlation between specific high-resolution features and associated echo types.

Results

Classification and distribution of echo types

The echo character along the western Svalbard margin varies from smooth, well-stratified, deep-penetrating reflectors to limited or absent acoustic penetration. The SBPs are divided into four major type classes—I, II, III and IV—on the basis of their echo character, as described below. Example SBPs for each echo type are shown in Figs. 1 and 2. The distribution of each echo type compiled using the SBPs, bathymetry and contour lines correlates with morphological features shown in Fig. 3. An example from the Kongsfjorden and Krossfjorden fjords is given in Fig. 4.

Type I demonstrates several diffuse, irregular, parallel internal reflectors with intermittent acoustically transparent units (Figs. 1a and 2c). This echo type is laterally discontinuous, is disrupted at the flanks of slopes with converging internal reflectors and is occasionally interrupted by a highly reflective seafloor. Type I deposits are found in undulating bathymetry with SBP reflections of a draped, ponded and mounded character, including acoustically transparent regions with sub-bottom penetration typically 5–25 ms. Type I is widespread on the continental slope, in shallower regions of the Yermak Plateau (Figs. 3 and 4). In Kongsfjorden and Krossfjorden, this echo type is described by Howe et al. (2003) as parallel, irregular-transparent reflectors. Gebhardt et al. (2011) have reported this as "facies types 3 & 4" (Table 1). This echo

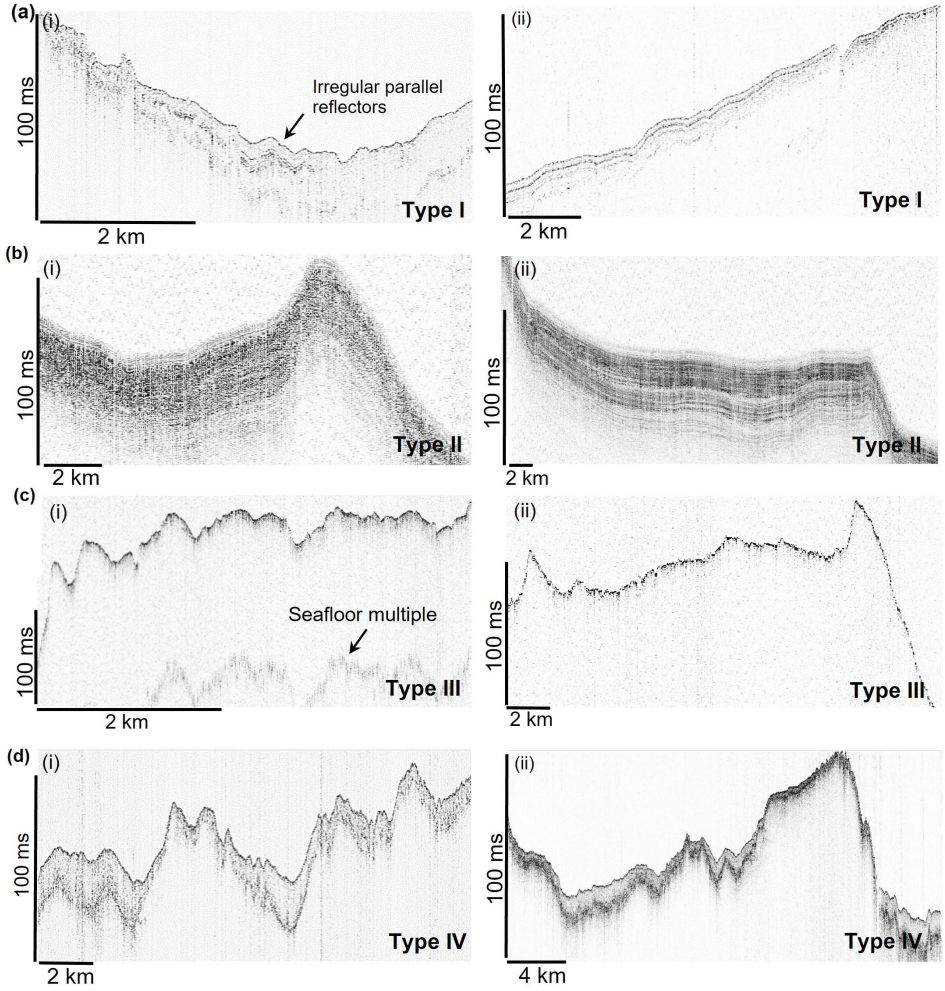

Fig. 1 Examples of TOPAS SBP lines showing the four different echo-character types. (a) Type I: thin, irregularly parallel, sub-bottom reflectors. (b) Type II: continuous, well-stratified, parallel, distinct sub-bottom reflectors. (c) Type III: continuous, highly reflective, absent of sub-bottom reflectors. (d) Type IV: single sub-bottom reflector with a transparent unit. See Figs. 3 and 4 for locations of example TOPAS profile lines.

type may reflect a range of depositional processes, with the lack of lateral continuity and reduced acoustic penetration attributed to less well-sorted sediment deposits. In fjords, Type I echoes are commonly associated with the lees of steep topographic slopes, so they seem to represent downslope sediment failures (e.g., GDFs).

Type II demonstrates several clear, well-stratified, laterally continuous, sub-bottom reflectors and deep acoustic penetration (Figs. 1b and 2c). The echo type is common on the continental slope, Vestnesa Ridge and Yermak Plateau and in Molloy Deep and isolated basins within the Kongsfjorden and Krossfjorden fjords (Figs. 3 and 4). This echo type is similar to Damuth's "Type IB" (Damuth 1978) and Pudsey & Howe's "Type V" (Pudsey & Howe 1998) and is associated with fine-grained, well-sorted, low-energy, slow-settling deposits. Gebhardt et al. (2011) reported this as "facies type 1 & 2" (Table 1). Howe et al. (2003) reported this echo character as occurring within Kongsfjorden and Krossfjorden, with the infilling seabed basins interpreted as Holocene (post-Little Ice Age) fine-grained sediments.

Type III shows a reflective, continuous, seabed echo with no sub-bottom reflections (Figs. 1c and 2a, b). Type III occurs most extensively on the continental shelf (Figs. 3 and 4) and on the upper slope, proximal to the mouths of the cross-shelf troughs of Kongsfjordrenna, Isfjordrenna and Bellsund and in a few isolated patches on steep slopes. This echo type is consistent with Damuth's "Type IA" (Damuth 1978) and Pudsey & Howe's "Type IV" (Pudsey & Howe 1998). Batchelor et al. (2016) reported this echo type as "Facies B" from the Yermak Plateau, and Gebhardt et al. (2011) reported this as "facies type 5" (Table 1). Here, we interpret this echo type as most likely associated with coarse-grained,

Citation: *Polar Research* 2025, *44*, 10847, http://dx.doi.org/10.33265/polar.v44.10847

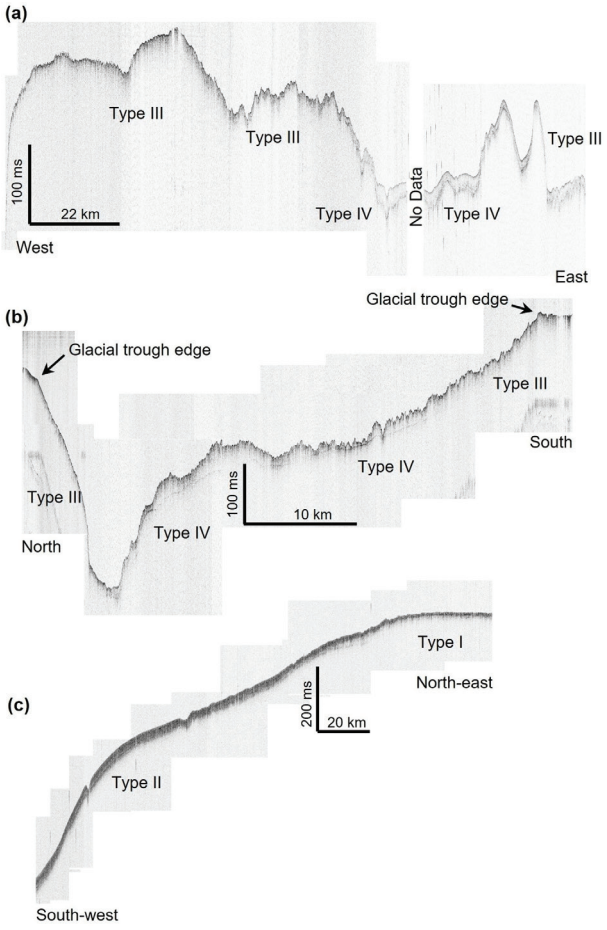

Fig. 2 SBP examples of four echo character types found on the western Svalbard margin. (a) Transect from shelf break along Kongsfjordrenna glacial trough to Kongsfjorden fjord. (b) Isfjordrenna glacial trough cross-section. (c) North-western Svalbard continental slope to Yermak Plateau. See Figs. 3 and 4 for SBP locations.

poorly-sorted sediments, potentially over-compacted by grounded ice or highly reflective bedrock outcrops, for example, in Kongsfjorden, occasionally with hyperbolic echo returns. Howe et al. (2003) recognized this same echo character, with its distribution consistent with identified bedrock outcrop locations in Kongsfjorden and Krossfjorden.

Type IV shows a sharp, uneven top surface, a single sub-bottom reflector with shallow seismic penetration and includes a homogeneous transparent acoustic signature unit between top and bottom surface reflectors (Figs. 1d and 2a, b). Type IV is restricted to the continental shelf, predominantly within Svalbard's glacial troughs and fjords (Figs. 3 and 4). This echo type character is interpreted as poorly sorted, coarse-grained glaciomarine material or glacigenic diamicton deposits. Gebhardt et al. (2011) reported this as "facies type 6" (Table 1).

Identification and distribution of geomorphological features

Morphological features interpreted using SBP lines and bathymetry include direct and indirect indicators of mass transport, erosion and gas or fluid flow seepage (Fig. 3). Acoustically, transparent lenses identified in the SBPr data from the margin are interpreted as GDFs, occurring predominately in depositional continental slope regions at the mouths of several cross-shelf glacial troughs, including that of Isfjordrenna (Fig. 3a, e). The limited spatial extent of the GDFs is why they are not classified as a separate acoustic echo type but instead overlay the predominant echo type of the region. GDFs are largely associated with trough mouth fans, forming distinct extensive progradation features on the shelf break and down the continental slope (Fig. 3a). The identification of an interpreted channel system originating immediately north of Vestnesa Ridge at the Kongsfjorden trough mouth fan was also recognized from the SBP and bathymetry data and slope-aspect mapping (Fig. 3a, b, d). Gas and fluid flow pockmarks and chimneys composed of mud are associated with Type II on the margin (Fig. 3a, c).

Discussion

This study of the western Svalbard margin has resulted in the broad-scale mapping of echo types and the depositional processes that are inferred from them. This approach has been taken previously on the Svalbard margin, notably by Batchelor et al. (2016) and Gebhardt et al. (2011), who all recognized a similar classification of acoustic types, although their focus was on the Yermak Plateau and northern Svalbard margin. The inferred depositional processes are described below as being high- or low-energy. High-energy processes include gravitationally induced mass wasting, such as debris flows, slides, slumps and turbidites. Low-energy processes include the slow settling of pelagites and hemipelagites as well as persistent bottom current sedimentation. The distribution of processes on the margin is illustrated through a simple conceptual model (Fig. 5).

High-energy downslope processes

On the continental slope and at the mouth of several cross-shelf troughs (e.g., Kongsfjordrenna, Isfjordrenna and Bellsund), the echo types all show the influence of high sedimentation rates, particularly during glacial episodes. The dominant echo type across these areas—Type III—is a highly reflective seabed with minimal acoustic penetration and occasional acoustically transparent lenses. These acoustic

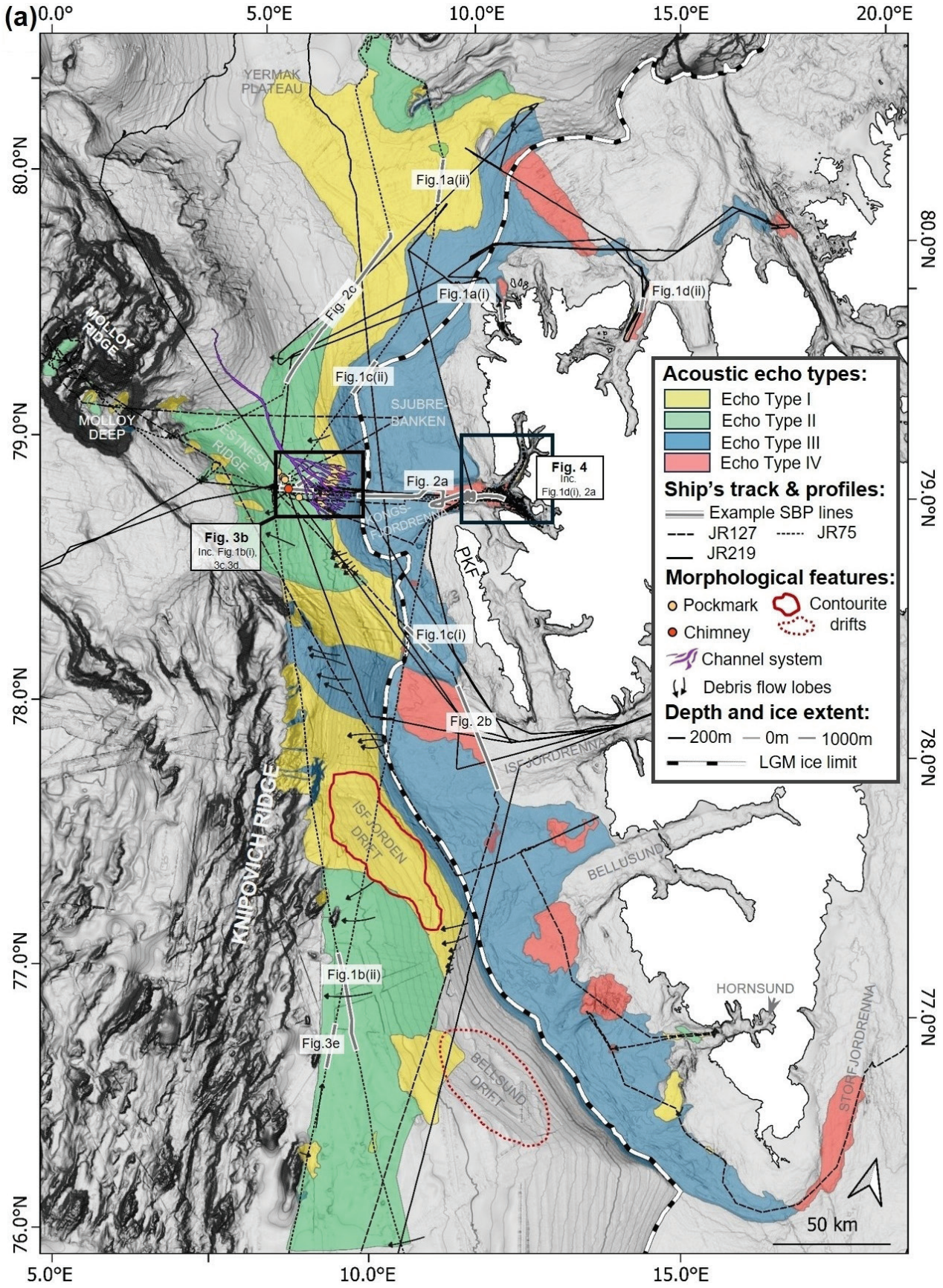

Citation: *Polar Research* 2025, *44*, 10847, http://dx.doi.org/10.33265/polar.v44.10847

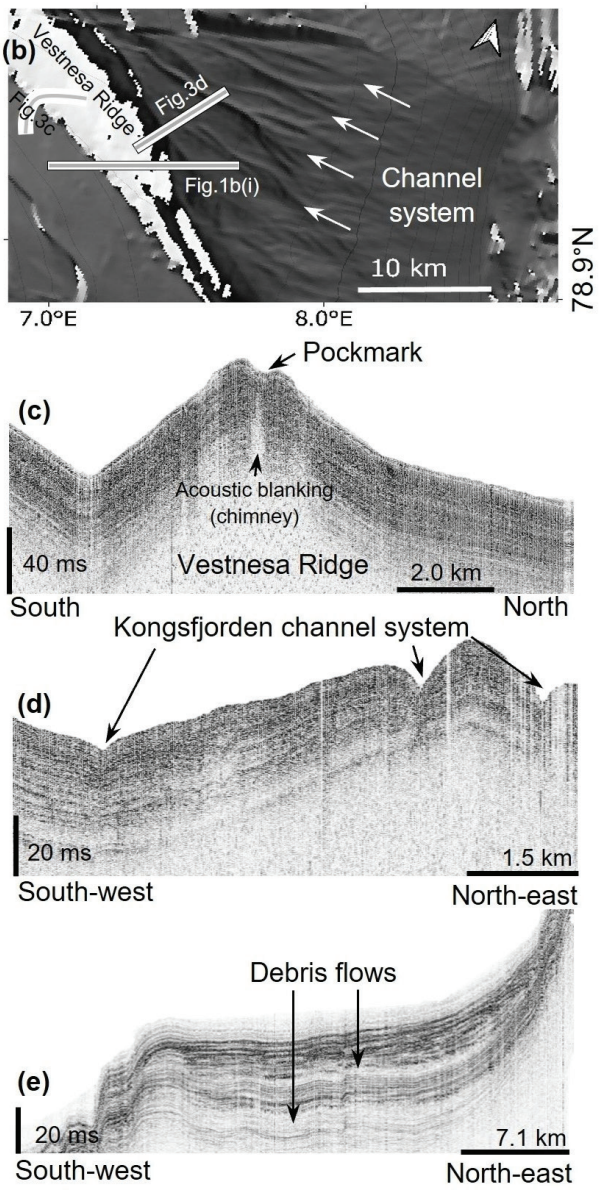

Fig. 3 (a) Echo character map of the western Svalbard margin showing the location and distribution of echo types I–IV (see Fig. 1). The maximum extent of the Svalbard–Barents Sea Ice Sheet, which occurred ca. 24 Kya, is drawn from Ottesen & Dowdeswell (2009) and Jessen et al. (2010). Bathymetry is from the IBCAO (Jakobsson et al. 2020). The Bellsund and Isfjorden drifts are identified on the basis of work by Rebesco et al. (2013). Prins Karls Foreland is abbreviated as PFK. (b) The KCS, interpreted on the basis of SBP, bathymetry data and interpretations by Forwick et al. (2015). The terrain aspect-slope mapping is from the IBCAO. (c) SBP of a pockmark at crest region of Vestnesa Ridge contourite drift. (d) SBP of the KCS, directly north of Vestnesa Ridge at the mouth of the Kongsfjordrenna glacial trough. (e) SBP of a debris flow lobe south-west of Svalbard in about 2240 m water depth.

characteristics are indicative of GDFs, the principal process constructing trough mouth fans. Vorren et al. (1998) and others have demonstrated that fast-flowing ice-streams can rapidly transport large volumes of glacigenic sediments, which can become modified sub-glacially as a deformable till layer (Boulton 1979). The prevalence of Type III in the cross-shelf regions is unsurprising, given the presence of pre-existing glacigenic transport pathways within the troughs across the shelf, delivering large volumes of sediment onto the slope and deeper areas of the margin.

A dominant feature of the northern Svalbard margin, with Type III in its upper section and Types I and II extending downslope, is a major downslope channel system. First described by Vogt et al. (1994), this channel system comprises a network of gullies and channels and was later called the KCS by Forwick et al. (2015). As with the GDF within Type III, the KCS originated from repeated erosion and mass wasting from a high sediment supply, most likely during glaciation. Downslope of the KCS and confined within the topographic boundaries of Sjubrebanken and Vestnesa Ridge, the system develops from multiple channels to a single channel persisting downslope to about 2840 m water depth. As with other channel systems on high-latitude margins (García et al. 2012), the KCS may have been most active during the LGM between about 14 and 23.3 Kya, coinciding with glacial sea-level lowstands and enhanced GDF input to the Kongsfjorden trough mouth fan by fast-flowing ice streams (Forwick et al. 2015).

The Type III echo character occurs across the shelf, with similar acoustic characteristics to those elsewhere on the Arctic and Subarctic continental shelves. Laberg & Vorren (1995) described similar GDF sampled from cores recovered from the Bjørnøya (Bear Island) trough mouth fan. In both shelf ice-stream and inter-ice-stream scenarios, a similar echo character—Type III—is observed. Ice sheet reconstructions by Landvik et al. (2005) suggest that these intermediate shelf banks were still inundated with ice, although sediment delivery was reduced compared to that of fast-flowing ice-stream settings, which transported less ice. As Type IV is mostly confined to the inner shelf regions of the glacial troughs, the trough mouth fans (Fig. 5) are here interpreted as originating from soft, deformable sediments at the base of mobile, fast-flowing ice streams.

Low-energy depositional and bottom-current influenced processes

In contrast to the high-energy depositional processes characterized by echo Types III and IV, low-energy processes, principally deriving from suspension and from the

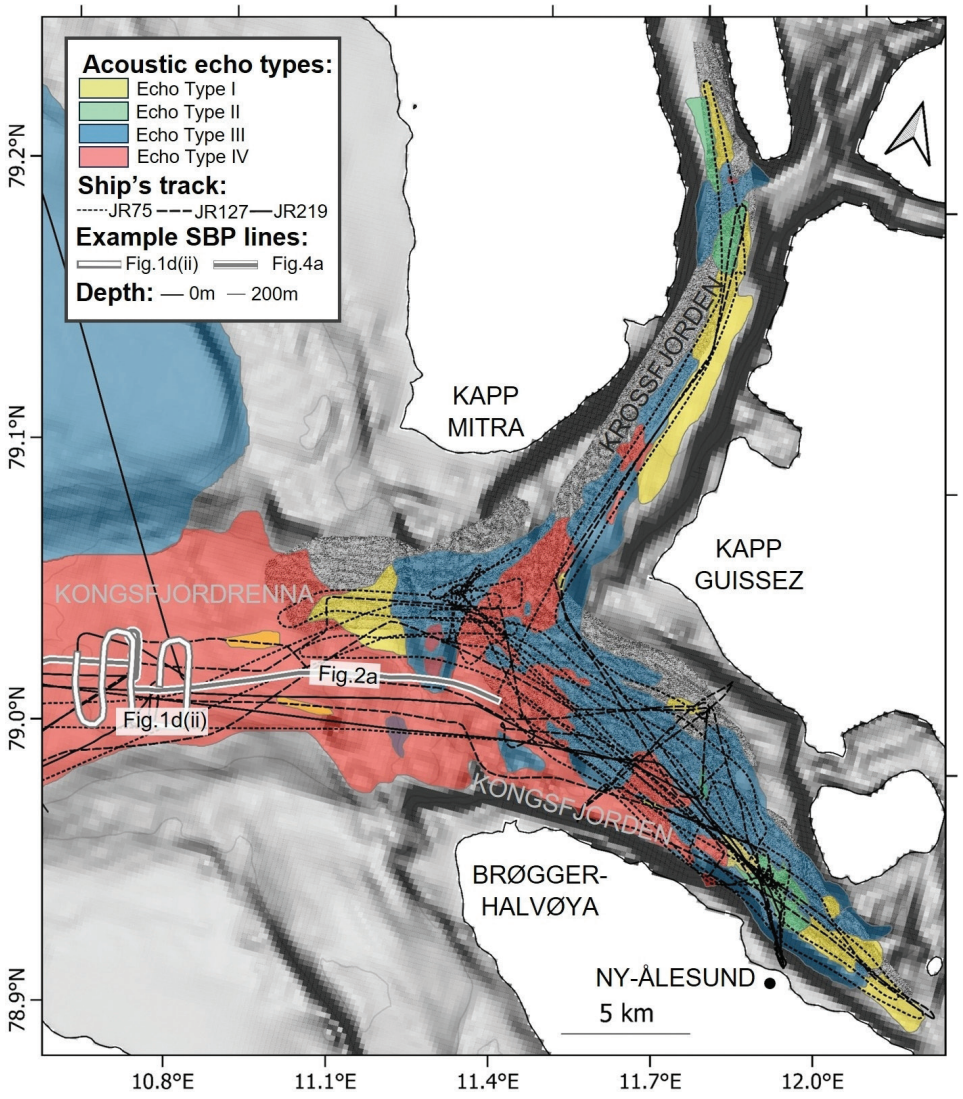

Fig. 4 Echo character map of the Kongsfjorden–Krossfjorden region. See Figs. 1, 2 and 3 for descriptions of echo types, ship tracks and SBP examples. Bathymetry from the IBCAO, with detailed bathymetric hill shading by Howe et al. (2003).

Table 1 Summary of echo character types and comparison with Gebhardt et al. (2011).

This study	Gebhardt et al. 2011	Acoustic characteristics (this study)
Type I	Facies type 3 & 4	Thin, irregular and parallel reflectors
Type II	Facies type 1 & 2	Continuous, well-stratified, parallel and distinct
Type III	Facies type 5	Continuous, highly reflective seabed echo
Type IV	Facies type 6	Single sub-bottom reflector with internal transparent units

influence of weak bottom-currents on the continental margin and rise, are also shown in the conceptual model (Fig. 5). Jessen et al. (2010) describe the onset of deglaciation at the shelf break as occurring about 20.5 Kya. In Kongsfjorden, the ice front had retreated east to the mouth of the fjord by about 16.6 Kya (Henriksen et al. 2014). Previous studies by MacLachlan et al. (2010) and Howe et al. (2003) provided an echo character stratigraphy within the Kongsfjorden and Krossfjorden area, identifying several echo types that are recognized in this present study. The well-stratified, continuous echo character of Type II occurs within isolated basins of the

Citation: *Polar Research* 2025, *44*, 10847, http://dx.doi.org/10.33265/polar.v44.10847

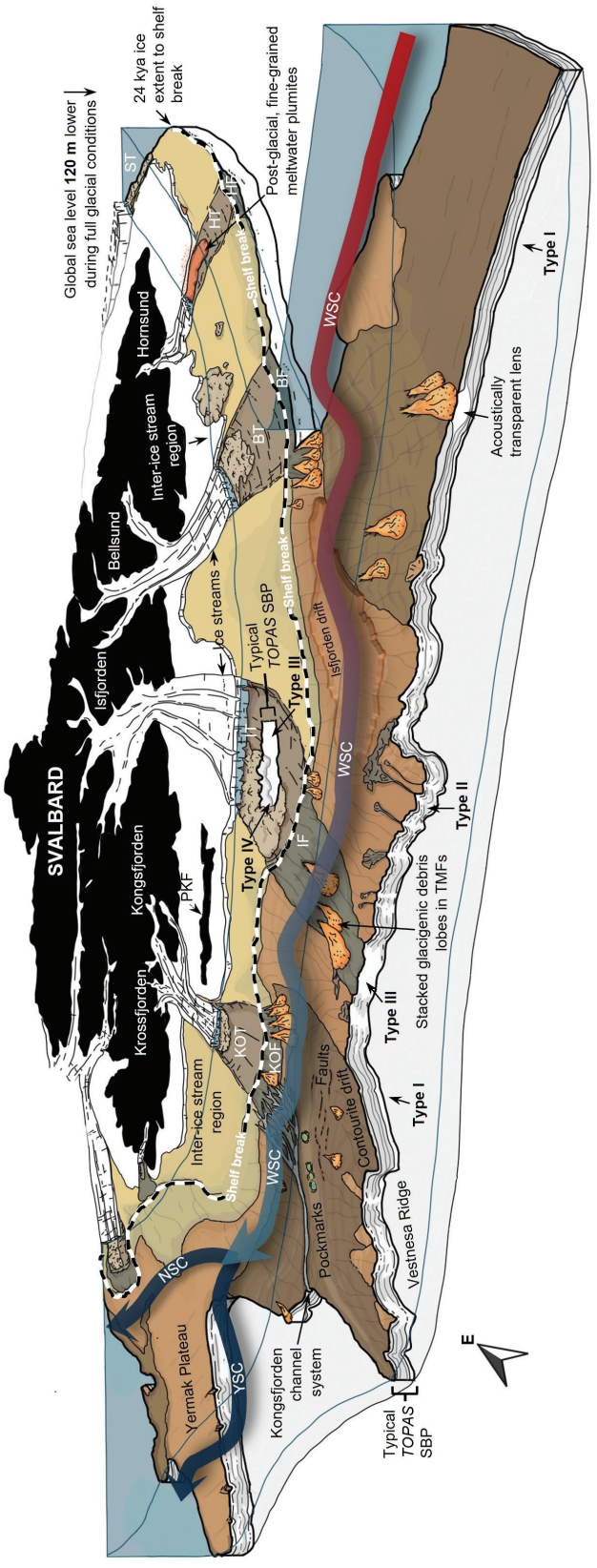

Fig. 5 A conceptual model of the deep-water processes on the western Svalbard margin informed by SBP echo characteristics. The margin is shown looking towards the east with major oceanographic currents shown in their simplified forms. During full glacial conditions, global sea level was about 120 m lower than shown (Rohling et al. 2009). Abbreviations: WSC, West Spitsbergen Current; YSC, Yermak Slope Current; NSC, North Spitsbergen Current; KOT, Kongsfjorden Trough; KOF, Kongsfjorden Fan; BT, Bellsund Trough; BF, Bellsund Fan; HT, Hornsund Trough; HF, Hornsund Fan; ST, Storfjorden Trough; PKF, Prins Karls Forland.

Kongsfjorden–Krossfjorden system. Howe et al. (2003) suggested these deposits accumulated during deglaciation under low-energy depositional environments, largely attributed to fine-grained direct suspension settling from the water column.

In southern Svalbard, in the Hornsund cross-shelf trough, echo character Type I (Fig. 5) is seen as irregularly parallel reflectors. These acoustically stratified sequences are interpreted as originating from a drape of fine-grained, possibly post-glacial deposits produced by sub-glacial meltwater plumes—what Hesse et al. (1997) call "plumites." Similar deposits were reported by Lucchi et al. (2013) further south, in the troughs of Storfjordrenna and Kveithola. Why the Hornsund Trough contains an occurrence of this echo character deposit whereas it is absent in similar glacial troughs to the north is uncertain. It could stem from persistent glacial ice within the Hornsund region, with sub-glacial meltwater plumes providing fine-grained sediments that were modified by bottom-currents within the cross-shelf trough.

Between the Kongsfjorden and Vestnesa Ridge, the echo character changes from Type III to Type II (Fig. 5). This change is characterized by numerous well-stratified, internal parallel reflectors with a much deeper sub-bottom acoustic penetration. The occurrence of echo Type II in these regions likely represents bottom current modification of sediments such as the development and maintenance of contourite drifts. Previous studies have reported well-stratified sediment drift deposits along the western Svalbard margin (e.g., Eiken & Hinz 1993; Howe et al. 2008). Rebesco et al. (2013) identify two drifts, the Isfjorden and Bellsund drifts. In this study, only the Isfjorden Drift occurs within the mapped region and within Type II echo character supporting the current-influenced interpretations of this echo type. Vogt et al. 1994 and others have recognized the influence of bottom-currents across the Vestnesa Ridge. The increased acoustic penetration and the soft, fine-grained sediment of the Vestnesa Ridge are consistent with findings in other studies of deposits of muddy-silty contourites and turbidites of Late Pleistocene age influenced by the West Spitsbergen Current (Eiken & Hinz 1993; Vogt et al. 1994; Howe et al. 2008).

Gas and fluid flow

The echo character map (Fig. 3) and the conceptual model (Fig. 5) also indicate seabed expressions of localized seabed fluid flow as pockmarks. In this study, pockmarks have been recognized in the eastern region of Vestnesa Ridge and are found to align along the crest axis with an absence of fluid flow seepage features on the ridge flanks. Widespread gas or fluid seepage from sediments occurs extensively all along on the western Svalbard margin (Mau et al. 2017), and numerous studies have reported pockmarks on the crest of Vestnesa Ridge (Vogt et al. 1994; Bünz et al. 2012; Plaza-Faverola et al. 2015). Pockmark distribution has been attributed to focused regions of sub-seabed fluid flow generated by fluid and gas flow around impermeable methane gas hydrate layers, a crystalline, ice-like compound composed of gas and water (Judd & Hovland 2007). In the case of the Vestnesa Ridge, this results in the funnelling of gas towards the crest of the ridge (Vanneste et al. 2005). Gas accumulation within the crest region is subsequently released via chimneys and pockmarks (Bünz et al. 2012). In the eastern part of Vestnesa Ridge, where pockmarks are identified, Plaza-Faverola et al. (2015) suggest this region lies within a zone of currently active sub-seabed faulting and gas seepage due to its proximity to the very slow spreading Molloy and Knipovich ridges. In the current study, pockmark identification along the entire ridge is hampered by the limited horizontal footprint of SBPr data. Cooke et al. (2023) identified pockmarks in the western section of the Vestnesa Ridge by using additional survey data. The few gas expulsion features, such as pockmarks in the deep sea, recognized in the current study, can be considered in the context of the more extensive systems described by Mau et al. (2017). These authors identify the "Svalbard Plume" as a much more widespread region of gas expulsion processes, extending to the shelf regions in the vicinity of the Hornsund Fracture Zone (Mau et al. 2017). It was not possible to identify gas expulsion features directly from the limited SBPr data within shelf regions in this study. This was likely due to the low or absent acoustic seafloor penetration in these regions, which make sub-bottom features such as chimneys difficult to distinguish.

Conclusions

This study illustrates the capability of broad-scale echo character mapping to provide an overview of depositional processes on a high-latitude margin. All the data in this study are archived legacy data, highlighting the importance of revisiting existing geophysical data sets.

Acknowledgements

The authors would like to thank Susi Woelz and Kevin Mackay (Earth Sciences New Zealand), Alice Fremand (British Antarctic Survey), Lewis Drysdale (Scottish Association for Marine Science) and Alex Tate

Citation: *Polar Research* 2025, *44*, 10847, http://dx.doi.org/10.33265/polar.v44.10847

(British Antarctic Survey) for their assistance in the data conversion and processing. Hannah Towns (Scottish Association for Marine Science) and Christian Armstrong provided valuable assistance with QGIS.

Funding

The data were collected as part of the Northern Seas and Oceans 2025 programmes (2002–2010), funded by the Natural Environment Research Council of the UK.

Disclosure statement

The authors report no conflict of interest.

Data availability statement

All data are archived at the UK Oceanographic Data Centre and are available there.

References

Aarseth I. 1997. Western Norwegian fjord sediments: age, volume, stratigraphy, and role as temporary depository during glacial cycles. *Marine Geology 143,* 39–53, doi: 10.1016/S0025-3227(97)00089-3.

Alexandropoulou N., Winsborrow M., Andreassen K., Plaza-Faverola A., Dessandier P.-A., Mattingsdal R., Baeten N. & Knies J. 2021. A continuous seismostratigraphic framework for the western Svalbard–Barents sea margin over the last 2.7 Ma: implications for the Late Cenozoic glacial history of the Svalbard–Barents sea ice sheet. *Frontiers in Earth Science 9*, 656–732, doi: 10.3389/feart.2021.656732.

Andersen E.S., Dokken T.M., Elverhoi A., Solheim A. & Fossen I. 1996. Late Quaternary sedimentation and glacial history of the western Svalbard continental margin. *Marine Geology 133,* 123–156, doi: 10.1016/0025-3227(96)00022-9.

Batchelor C.L., Dowdeswell J.A., Jakobsson M., Hogan K.A. & Gebhardt A.C. 2016. Landform assemblage produced by ice-grounding events on the Yermak Plateau. In J.A. Dowdeswell et al. (eds.): *Atlas of submarine glacial landforms: modern, Quaternary and ancient.* Pp. 329–332. London: The Geological Society.

Bensi M., Kovacevic V., Langone L., Aliani S., Ursella U., Goszczko I., Soltwedel T., Skogseth R., Nilsen F., Deponte D., Mansutti P., Laterza R., Rebesco M., Rui L., Lucchi R.G., Wahlin A., Viola A., Beszcynska-Möller A. & Rubino A. 2019. Deep flow variability offshore south-west Svalbard (Fram Strait). *Water 11*, article no. 683, doi: 10.3390/w11040683.

Boulton G.S. 1979. Processes of glacier erosion on different substrata. *Journal of Glaciology 23*, 15–38, doi: 10.3189/S0022143000029713.

Bünz S., Polyanov S., Vadakkepuliyambatta S., Consolaro C. & Mienert J. 2012. Active gas venting through hydrate-bearing sediments on the Vestnesa Ridge, offshore W-Svalbard. *Marine Geology 332*, 189–197, doi: 10.1016/j.margeo.2012.09.012.

Chauhan T., Noormets R. & Rasmussen T.L. 2016. Glaciomarine sedimentation and bottom current activity on the north-western and northern continental margins of Svalbard during the late Quaternary. *Geo-Marine Letters 36*, 81–99, doi: 10.1007/s00367-015-0430-6.

Cooke F., Plaza-Faverola A., Bunz S., Sultan N., Ramachandran H., Bedle H., Patton H., Singhroha S. & Knies J. 2023. Sedimentary deformation relating to episodic seepage in the last 1.2 million years: a multi-scale seismic study from the Vestnesa Ridge, eastern Fram Strait. *Frontiers in Earth Science 11*, article no. 1188737, doi: 10.3389/feart.2023.1188737.

Damuth J.E. 1975. Echo character of the western equatorial Atlantic floor and its relationship to the dispersal and distribution of terrigenous sediments. *Marine Geology 18*, 17–45, doi: 10.1016/0025-3227(75)90047-X.

Damuth J.E. 1978. Echo character of the Norwegian–Greenland Sea: relationship to Quaternary sedimentation. *Marine Geology 28*, 1–36, doi: 10.1016/0025-3227(78)90094-4.

Damuth J.E. 1980. Quaternary sedimentation processes in the South China Basin as revealed by echo-character mapping and piston-core studies. In D.E. Hayes (ed.): *The tectonic and geologic evolution of Southeast Asian seas and islands*. Pp. 105–125. Washington, DC: American Geophysical Union.

Damuth J.E. & Hayes D.E. 1977. Echo character of the east Brazilian continental margin and its relationship to sedimentary processes. *Marine Geology 24*, 73–95, doi: 10.1016/0025-3227(77)90002-0.

Davies T.A., Bell T., Cooper A.K., Josenhans H., Polyak L., Solheim A., Stoker M.S. & Stravers J.A. (eds.) 1999. *Glaciated continental margins: an atlas of acoustic images*. London: Chapman and Hall.

Domzig A., Gaullier V., Giresse P., Pauc H., Deverchere J. & Yelles K. 2009. Deposition processes from echo-character mapping along the western Algerian margin (Oran–Tenes), western Mediterranean. *Marine and Petroleum Geology 26*, 673–694, doi: 10.1016/j.marpetgeo.2008.05.006.

Dowdeswell J.A., Elverhøi A. & Spielhagen R. 1998. Glacimarine sedimentary processes and facies on the Polar North Atlantic margins. *Quaternary Science Reviews 17*, 243–272, doi: 10.1016/S0277-3791(97)00071-1.

Eiken O. & Hinz K. 1993. Contourites in the Fram Strait. *Sedimentary Geology 82*, 15–32, doi: 10.1016/0037-0738(93)90110-Q.

Elverhøi A., Dowdeswell J.A., Funder S., Mangerud J. & Stein R. 1998. Glacial and oceanic history of the polar North Atlantic margins: an overview. *Quaternary Science Reviews 17*, 1–10, doi: 10.1016/S0277-3791(97)00073-5.

Forwick M., Laberg J.S., Hass H.C. & Osti G. 2015. The Kongsfjorden channel system offshore NW Svalbard: downslope sedimentary processes in a contour-current-dominated setting. *Arktos: The Journal of Arctic Geosciences 1*, article no. 17, doi: 10.1007/s41063-015-0018-4.

García M., Dowdeswell J.A., Ercilla G. & Jakobsson M. 2012. Recent glacially influenced sedimentary processes on the East Greenland continental slope and deep Greenland Basin. *Quaternary Science Reviews 49*, 64–81, doi: 10.1016/j.quascirev.2012.06.016.

Gebhardt A.C., Jokat W., Niessen F., Matthiessen J., Geissler W.H. & Schenke H.-W. 2011. Ice sheet grounding and iceberg plow marks on the northern and central Yermak Plateau revealed by geophysical data. *Quaternary Science Reviews 30*, 1726–1738, doi: 10.1016/j.quascirev.2011.03.016.

Hamilton E.L. 1956. Low sound velocities in high-porosity sediments. *The Journal of the Acoustical Society of America 28*, 16–19, doi: 10.1121/1.1908208.

Henriksen M., Alexanderson H., Landvik J.Y., Linge H. & Peterson G. 2014. Dynamics and retreat of the Late Weichselian Kongsfjorden ice stream, NW Svalbard. *Quaternary Science Reviews 92*, 235–245, doi: 10.1016/j.quascirev.2013.10.035.

Hesse R., Khodabakhsh S., Klaucke I. & Ryan W.B.F. 1997. Asymmetrical turbid surface-plume deposition near ice-outlets of the Pleistocene Laurentide ice sheet in the Labrador Sea. *Geo-Marine Letters 17*, 179–187, doi: 10.1007/s003670050024.

Howe J.A., Moreton S., Morri C. & Morris P. 2003. Multibeam bathymetry and the depositional environments of Kongsfjorden and Krossfjorden, western Spitsbergen, Svalbard. *Polar Research 22*, 301–316, doi: 10.3402/polar.v22i2.6462.

Howe J.A., Shimmield T., Harland R. & Eyles N. 2008. Late Quaternary contourites and glaciomarine sedimentation in the Fram Strait. *Sedimentology 55*, 179–200, doi: 10.1111/j.1365-3091.2007.00897.

Hughes A.L.C., Gyllencreutz R., Lohne Ø.S., Mangerud J. & Svendsen J.I. 2016. The last Eurasian ice sheets—a chronological database and time-slice reconstruction, DATED-1. *Boreas 45*, 1–45, doi: 10.1111/bor.12142.

Jakobsson M., Backman J., Rudels B., Nycander J., Frank M., Mayer L., Jokat W., Sangiori F., O'Regan M., Brinkhuis H., King J. & Moran K. 2007. The early Miocene onset of a ventilated circulation regime in the Arctic Ocean. *Nature 447*, 986–990, doi: 10.1038/nature05924.

Jakobsson M., Gyllencreutz R. Mayer L.A. Dowdeswell J.A. Canals M. Todd B.J. Dowdeswell E.K. Hogan K.A. & Larter R.D. 2016. Mapping submarine glacial landforms using acoustic methods. In J.A. Dowdeswell et al. (eds.): *Atlas of submarine glacial landforms: modern, Quaternary and ancient*. Pp. 17–40. London: The Geological Society.

Jakobsson M., Mayer L.A., Bringensparr C., Castro C.F., Mohammad R., Johnson P., Ketter T., Accettella D., Amblas D., An L., Arndt J.E., Canals M., Casamor J.L., Chauche N., Coakley B., Danielson S., Demarte M., Dickson M.-L., Dorschel B., Dowdeswell J.A., Druetter S., Fremand A.C., Gallant D., Hall J.K., Hehemann L., Hodnesdal H., Hong J., Ivaldi R., Kane E., Klaucke I., Krawczyk D.W., Kristoffersen Y., Kuipers B.R., Millan R., Masetti G., Morlighem M., Noormets R., Prescott M.M., Rebesco M., Rignot E., Semiletov I., Tate A.J., Travaglini P., Velicogna I., Weatherall P., Weinrebe W., Willis J.K., Wood M., Zarayskaya Y., Zhang T., Zimmermann M. & Zinglersen K.B. 2020. The International Bathymetric Chart of the Arctic Ocean Version 4.0. *Scientific Data* 7, article no. 176, doi: 10.1038/s41597-020-0520-9.

Jessen S.P., Rasmussen T.L., Nielsen T. & Solheim A. 2010. A new Late Weichselian and Holocene marine chronology for the western Svalbard slope 30,000-0 cal years BP. *Quaternary Science Reviews 29*, 1301–1312, doi: 10.1016/j.quascirev.2010.02.020.

Judd A.G. & Hovland M. 1992. The evidence of shallow gas in marine sediments. *Continental Shelf Research 12*, 1081–1095, doi: 10.1016/0278-4343(92)90070-Z.

Judd A.G. & Hovland M. 2007. *Seabed fluid flow: the impact of geology, biology and the marine environment*. Cambridge: Cambridge University Press.

Laberg J.S. & Vorren T.O. 1995. Late Weichselian submarine debris flow deposits on the Bear Island Trough mouth fan. *Marine Geology 127*, 45–72, doi: 10.1016/0025-3227(95)00055-4.

Landvik J., Ingolfsson O., Mienert J., Lehman S., Solheim A., Elverhøi A. & Ottesen D. 2005. Rethinking Late Weichselian ice-sheet dynamics in coastal NW Svalbard. *Boreas 34*, 7–24, doi: 10.1080/03009480510012809.

Lucchi R.G., Camerlenghi A., Rebesco M., Colmenero-Hidalgo E., Sierro F.J., Sagnotti L., Urgeles R., Melis R., Morigi C., Bárcena M.-A., Giorgetti G., Villa G., Persico D., Flores J.A., Rigual-Hernández A.S., Pedrosa M.T., Macri P. & Caburlotto A. 2013. Postglacial sedimentary processes on the Storfjorden and Kveithola Trough mouth fans: significance of extreme glacimarine sedimentation. *Global and Planetary Change 111*, 309–326, doi: 10.1016/j.gloplacha.2013.10.008.

Lucchi R.G., St John K.E.K., Ronge T.A. & the Expedition 403 Scientists. 2024. *Expedition 403 preliminary report: eastern Fram Strait paleo-archive*. College Station, TX: International Ocean Discovery Program.

MacLachlan S.E., Howe J.A. & Vardy M.E. 2010. Morphodynamic evolution of Kongsfjorden–Krossfjorden, Svalbard, during the late Weichselian and Holocene. In J.A. Howe et al. (eds.): *Fjord systems and archives*. Pp. 195–205. London: The Geological Society.

Maestro A., Gallastegui A., Moreta M., Llave E., Bohoyo F. & Duret M. 2021. Echo character distribution in the Cantabrian Margin and the Biscay Abyssal Plain. *Journal of Maps 17*, 547–556, doi: 10.1080/17445647.2021.1973917.

Mau S., Römer M., Torres M.E., Bussmann I., Pape T., Damm E., Geprägs P., Wintersteller P., Hsu C.W., Loher M. & Bohrmann G. 2017. Widespread methane seepage along the continental margin off Svalbard—from Bjørnøya to Kongsfjorden. *Nature Scientific Reports 7*, article no. 42997, doi: 10.1038/srep42997.

McCave I.N. 2002. Sedimentary settings on continental margins—an overview. In G. Wefer et al. (eds.): *Ocean margin systems*. Pp. 1–14. Berlin: Springer.

Nilsen F.R., Skogseth R., Vaardal-Lunde J. & Inall M.E. 2016. A simple shelf circulation model: intrusion of Atlantic Water on the West Spitsbergen Shelf. *Journal of Physical Oceanography 46*, article no. 12091230, doi: 10.1175/JPO-D-15-0058.1.

Orsi T.H. & Dunn D.A. 1991. Correlations between sound velocity and related properties of glacio-marine sediments: Barents Sea. *Geo-Marine Letters 11*, 79–83, doi: 10.1007/BF02431033.

Ottesen D. & Dowdeswell J.A. 2009. An inter-ice-stream glaciated margin: submarine landforms and a geomorphic model based on marine-geophysical data from Svalbard. *Geological Society of America Bulletin 121*, 1647–1665, doi: 10.1130/B26467.1.

Plaza-Faverola A., Bünz S. Johnson J.E., Chand S., Knies J., Mienert J. & Franek P. 2015. Role of tectonic stress in seepage evolution along the gas hydrate-charged Vestnesa Ridge, Fram Strait. *Geophysical Research Letters 42*, 733–742, doi: 10.1002/2014GL062474.

Pudsey C.J. & Howe J.A. 1998. Quaternary history of the Antarctic Circumpolar Current: evidence from the Scotia Sea. *Marine Geology 148*, 83–112, doi: 10.1016/S0025-3227(98)00014-0.

Rebesco M., Wåhlin A., Laberg J., Schauer U., Beszczynska-Möller A., Lucchi R.G., Noormets R., Accettella D., Zarayskaya Y. & Diviacco P. 2013. Quaternary contourite drifts of the western Spitsbergen margin. *Deep-Sea Research Part I 79*, 156–168, doi: 10.1016/j.dsr.2013.05.013.

Rohling E.J., Grant K., Bolshaw M., Roberts A.P., Siddall M., Hemleben C. & Kucera M. 2009. Antarctic temperature and global sea level closely coupled over the past five glacial cycles. *Nature Geoscience 2*, 500–504, doi: 10.1038/ngeo557.

Rudels B., Meyer R., Fahrbach E., Ivanov V.V., Østerhus S., Quadfasel D., Schauer U., Tverberg V. & Woodgate R.A. 2000. Water mass distribution in Fram Strait and over the Yermak Plateau in summer 1997. *Annales Geophysicae 18*, 687–705, doi: 10.1007/s00585-000-0687-5.

Solheim A., Faleide J.I., Andersen E.S., Elverhoi A., Forsberg C.F., Vanneste K., Uenzelmann-Neben G. & Channell J.E.T. 1998. Late Cenozoic seismic stratigraphy and glacial geological development of the east Greenland and Svalbard–Barents Sea continental margins. *Quaternary Science Reviews 17*, 155–184, doi: 10.1016/S0277-3791(97)00068-1.

Vanneste M., Guidard S. & Mienert J. 2005. Bottom-simulating reflections and geothermal gradients across the western Svalbard margin. *Terra Nova 17*, 510–516, doi: 10.1111/j.1365-3121.2005.00643.

Vogt P.R., Crane K., Sundvor E., Max M.D. & Pfirman S.L. 1994. Methane-generated(?) pockmarks on young, thickly sedimented oceanic crust in the Arctic: Vestnesa Ridge, Fram Strait. *Geology 22*, 255–258, doi: 10.1130/0091-7613.

Vorren T.O., Laberg J.-S., Blaume F., Dowdeswell J., Kenyon N., Mienert M., Ruhmohr J. & Werner F. 1998. The Norwegian–Greenland Sea continental margins: morphology and late Quaternary sedimentary processes and environment. *Quaternary Science Reviews 17*, 273–302, doi: 10.1016/S0277-3791(97)00072-3.